Effect of anisotropy on the thermal volume changes of the Callovo–Oxfordian claystone

Philipp Braun, Pierre Delage, Siavash Ghabezloo, Jean Sulem, Nathalie Conil

Effect of transverse isotropy on the thermal volume changes of shales: insight from the Callovo-Oxfordian claystone

Géotechnique Letters 2019, doi.org/10.1680/jgele.19.00045.

Braun Philipp, Delage Pierre, Ghabezloo Siavash, Sulem Jean
Navier-CERMES, Ecole des Ponts ParisTech, Marne la Vallée, France
Conil Nathalie
Andra, Bure, France

Abstract

An accurate monitoring of axial and radial thermal strains of a specimen of the Callovo-Oxfordian claystone, heated under constant confining stress condition close to that prevailing in the Bure Underground Research Laboratory at 490 m depth, evidenced a particular behaviour feature. The effect of the transverse isotropy of the claystone on thermal strains was confirmed, but it was also shown that the thermo-elasto-plastic overall volumetric response was mainly due to the axial response, in which some influence of the adsorbed water is suspected. Conversely, the reversible radial response observed along a temperature cycle could be modelled through a simple homogenisation method that confirmed that it was governed by the thermo-elastic expansion/contraction response of the constitutive minerals. Hence, the simultaneous occurrence of elastic thermal radial strains and elasto-plastic thermal axial strains was evidenced.

Keywords

Anisotropy, clays, fabric/structure of soils, Radioactive waste disposal, temperature effects

List of notations

w Water content
ϕ Porosity
σ Stress
p Mean stress
u Pore water pressure
α_i Linear thermal expansion coefficient of mineral *i*
$\alpha_{d,\,ax}$ Drained linear thermal expansion coefficient in axial direction, perpendicular to bedding
$\alpha_{d,\,rad}$ Drained linear thermal expansion coefficient in radial direction, parallel to bedding
P_i Proportion of mineral *i*
V Specimen volume
t Time
T Temperature

Introduction

The assessment of the thermal impact of heat-generating radioactive wastes in clays, claystones and shales has been investigated in Europe, with particular attention paid to the Boom clay, a stiff clay from Belgium (e.g. Hueckel and Baldi 1990, Sultan et al. 2002), and two claystones, the Opalinus Clay in Switzerland (e.g. Monfared et al. 2011, Favero et al. 2016) and the Callovo-Oxfordian claystone in France (e.g. Mohajerani et al. 2014, Menaceur et al. 2015a and b, Zhang et al. 2017 (their characteristics are given in Gens 2013). In all concepts, the maximum temperature allowed in the host rock is 100°C. Few data are available on the thermal volume changes of claystones.

On both the Opalinus Clay (Monfared et al. 2011) and the Callovo-Oxfordian claystone (Belmokhtar et al. 2017a), thermo-elastic volume changes have been observed at temperatures smaller than the highest temperature experienced during the geological history of the claystone (estimated around 50°C in the COx, Blaise et al. 2014), whereas plastic thermal contraction occurred at higher temperature. The physical mechanisms governing this contraction is poorly understood, most authors suspecting it to be due to the release of adsorbed water within the clay fraction.

Thermal volume changes have often been monitored in a global way, with no consideration on the effects of the transverse isotropy that results, in clays and claystones, from the preferential orientation of clay platelets along the bedding plane. In this paper, these effects have been further investigated on the Callovo-Oxfordian claystone thanks to an accurate monitoring of the axial and radial strains by using strain gauges.

2. Material and methods

The Callovo-Oxfordian claystone

The Callovo-Oxfordian (COx) claystone is a low permeability sedimentary rock (k smaller than 10^{-20} m^2, Escoffier et al. 2005, Mohajerani et al. 2011, Menaceur et al. 2015b) deposited 155 millions years ago on the eastern fringe of the Parisian basin. At 490 m, in the middle of the COx layer where the Bure Underground Research Laboratory (URL) is located, the claystone is composed of a clay matrix (average 42% +/-11%) in which are embedded 30% carbonates, 25% quartz and a small fraction of feldspar (Conil et al. 2018). The clay matrix is composed of platelets preferably oriented along the bedding plane, providing some degree of anisotropy to the texture. It contains 10-24% mixed-layer illite/smectite (with 50 – 70% smectite, Yven et al. 2007), 17-21% illite, 3-5% kaolinite, 2-3% chlorite (Gaucher et al., 2004). At the URL, the stress state is (Wileveau et al. 2007, Conil et al. 2018): total vertical stress σ_v = 12 MPa, major horizontal stress σ_H = 16 MPa, minor horizontal stress σ_h = 12 MPa, (hydrostatic) pore pressure u = 4.9 MPa, resulting in a mean Terzaghi effective stress $p' = (\sigma_v + \sigma_H + \sigma_h)/3 - u$ = 8.4 MPa and a Biot mean average effective stress of 8.9 MPa (with a Biot coefficient of 0.9, Belmokhtar et al. 2017b).

The specimens come from horizontal cores EST53650 and EST57185 (80 mm diameter) from the Bure URL. Specimens were diamond cored perpendicular to the bedding plane with a diameter of 38 mm and cut at a length of 10 mm with a diamond saw. The average water content of both cores (w = 7.7 %) was determined on cuttings after oven-drying during 48 h at 105°C. The average porosity of both cores (ϕ = 18.1 %) was determined by hydrostatic weighing on some cuttings in unflavoured hydrocarbon, providing a degree of saturation of 93.9 %. An average suction of 20.1 MPa was measured with a dew point potentiometer (WP4C, Decagon Devices), indicating good specimen preservation with minimised evaporation after coring.

Thermal isotropic compression cell

The used thermal isotropic compression cell (Figure 1, Belmokhtar et al. 2017a, b and Braun et al. 2019) accommodates the 38mm diameter porous disc. It is connected to two pressure-volume controllers (PVC, GDS Brand) for confining pressure (using oil) and back-pressure (using a synthetic water with same pore water salt composition as that of the COx, Table 1). Axial and radial strains were monitored by strain gauges glued parallel and perpendicular to bedding. Thermal effects were compensated by means of a reference gauge glued to a metal dummy piece placed close to the specimen, supporting the same stress/temperature path. A heating belt wrapped around the cell allowed for temperature control (+/- 0.1°C) and temperature was measured by a thermocouple inside the cell. Drainage was ensured through a thin porous metal disk at the specimen bottom. Given that specimens were slightly desaturated due to coring, storage and trimming (Monfared et al. 2011, Ewy 2015), they were placed on the dry porous disk and loaded to in-situ stress conditions (under constant water content, with only air escaping) at a rate of 0.1 MPa/mn. The ducts and porous disk were put under vacuum prior to be filled with synthetic pore water, injected under a pressure of 100 kPa. Water saturation was hence ensured under stress conditions equal or larger than in-situ, so as to minimize swelling and damage and to fit as much as possible with in-situ conditions.
Instead of applying a drained temperature increase at low constant rate (Belmokhtar et al. 2017a), it was preferred to increase temperature by step and to wait for the dissipation of induced thermal pore pressure (see Delage et al. 2000 and Braun et al. 2019 for more details). The strain response, once stabilised, is representative of the drained thermal response of the claystone.

3. Experimental data

Four tests were performed. Samples ISO1 and 4 were loaded under 10 MPa and samples ISO2 to 4 under 8 MPa. Once the specimen in contact with water, both the back and the confining pressures were simultaneously and equally increased to reach a final pore pressure of 4 MPa, resulting in an effective isotropic confining stress of 10 MPa ($\sigma - u$ = 14 – 4 MPa) for ISO1 and 4, and of 8 MPa ($\sigma - u$ = 12 – 4 MPa) for ISO2 and 3, not far from the in-situ stress conditions.
Tests ISO2 and ISO3 were carried out according to a two stages protocol (like in Sultan et al. 2002), by keeping Valve V1 (Figure 1) opened, with a 4 MPa back-pressure applied by the PVC at the specimen bottom. The fast temperature increase resulted in an undrained volume and pore pressure increase, followed by a progressive volume decrease due to pore pressure dissipation. In tests ISO3 and 4, valve V1 was initially closed during 5 hours, prior to be opened and to allow the dissipation of thermal pore pressures during 20h.
The changes in volume with respect to temperature of tests ISO 3 and 4, run under constant Terzaghi effective mean stresses of 8 and 10 MPa and maximum temperatures of 90 and 80°C, respectively, are presented in Figure 2. Unfortunately, whereas the horizontal strain gauges work properly in all 4 cases, some problems were met with vertical strain gauges in tests ISO 1 and 2, and the corresponding bulk volume changes could not be monitored.
Both curves exhibit comparable trends, with however some differences due to the fact that small temperature cycles have been performed at 50°C and 70°C in test ISO4. Once the maximum temperature attained, both cooling curves are parallel. As already observed by Belmokhtar et al. (2017a), the thermal volume change curves start by a thermal expansion, defined by a slope close to that observed during the cooling phase afterwards, indicated by the two parallel straight dotted lines in Figure 2. The initial thermal expansion is followed by contraction, with an expansion/ contraction transition observed in both tests between 50 and 60°C, close to the maximum temperature experienced during the geological history of the COx, i.e. 50°C +/- 5°C (Blaise et al.

2014). A similar trend was also observed on the Opalinus Clay by Monfared et al. (2011), with a maximum temperature of 80°C.

Data from all tests are presented in terms of axial and radial strains in Figure 3, that evidences a significant difference between strains perpendicular (axial) and parallel (radial) to bedding. The radial strain response to the temperature cycle is fairly reversible, at least for tests ISO1, 2 and 4, providing an average radial thermal expansion coefficient $\alpha_{d,\,rad}$ = 0.51 x10^{-5} °C^{-1}. Conversely, contraction and irreversibility is quite apparent in the axial (and comparable) responses of tests ISO 3 and 4. The slope obtained along the cooling phase of tests ISO3 and 4 are quite close, giving a smaller axial thermal expansion coefficient $\alpha_{d,\,ax}$ = 0.21 x10^{-5} °C^{-1}.

4. Discussion

The data of tests ISO 3 and 4 in Figure 2 confirm the similarity of the thermal volume response between the COx and Opalinus claystones, with an initial thermo-elastic expansion followed by thermo-plastic contraction, once the highest temperature experienced by the claystone has been reached. However, the accurate measurements of strains parallel and perpendicular to bedding presented in Figure 3 provide further information on the effects of the anisotropy due to the preferable orientation of clay platelets along the bedding direction. A remarkably reversible strain response parallel to bedding is observed along the temperature cycles in tests ISO 1, 2 and 4 (whereas some degree of irreversibility is observed in test ISO3), indicating a thermo-elastic response characterised by a slope providing the linear thermal expansion coefficient parallel to bedding $\alpha_{d,rad}$ = 0.51 x 10^{-5} °C^{-1}. This value can be compared to the literature data reported in Table 2, that presents the thermal dilation coefficient of quartz, calcite and feldspar, together with those, parallel and perpendicular to bedding, of (dry) muscovite, a sheet silicate comparable to illite and smectite.

The value of 0.35 x 10^{-5} °C^{-1} parallel to bedding provided by McKinstry (1965) is close to our value ($\alpha_{d,rad}$ = 0.51 x 10^{-5} °C^{-1}). A more precise estimation can be made by using a quite simplified homogenisation technique based on the schematic representation of the grains embedded in a clay matrix, presented in Figure 4. Along the radial direction, one can consider that the global thermal radial dilation $\alpha_{d,rad}$ is the sum of those of the various minerals, provided their effect is weighted by their proportion (P_i), resulting in the following expression:

$$\alpha_{d,rad} = \sum_1^3 \alpha_i \, P_i \qquad (1)$$

Adopting the P_i and α_i data of Table 2 (parallel for muscovite), one obtains a value $\alpha_{d,rad}$ = 0,58 x 10^{-5} °C^{-1}, fairly close to the measured value of 0,51 x 10^{-5} °C^{-1}. This good correspondence confirms that the driving force of thermal strain parallel to bedding is the reversible thermo-elastic dilation of minerals.

Things are less evident when considering the axial thermal response, for which the same simplified approach provides a larger value of 1.18 x 10^{-5} °C^{-1} (because of the larger thermal dilation of muscovite perpendicular to bedding), whereas the slope of the cooling curves of tests ISO3 and 4 provide an average smaller value $\alpha_{d,\,ax}$ = 0.21 x10^{-5} °C^{-1}. Due to the preferred sub-horizontal orientation of the clay platelets, it is suspected that the thermo-elastic volume changes (observed along the cooling path) are no longer only dependent of the mineral thermal expansion/contraction, but also influenced by the thermal response of the adsorbed water molecules, either within the platelets or in the inter-platelets porosity (see Menaceur et al. 2016). The reason why this results in a smaller coefficient is not yet fully understood. The thermo-plastic contraction observed at higher temperature response is poorly documented in the literature.

Conclusion

Thermal tests conducted on specimens of the Callovo-Oxfordian claystone under constant effective stress confirmed the trend already observed on both the Opalinus Clay and the Callovo-Oxfordian claystone, i.e. a drained thermo-elastic expansion followed by a thermo-plastic contraction occurring once the maximum temperature experienced during the geological history has been overpassed.

The accurate monitoring of axial and radial strains by means of strain gauges confirmed the effects of the structural anisotropy of the Callovo-Oxfordian claystone. It was shown that the overall thermo-elasto-plastic volumetric behaviour was mainly due to the axial response (in which adsorbed water molecules appear to be involved), whereas the radial response remained thermo-elastic, only governed by the expansion coefficients of the constitutive minerals. This new observation illustrates quite a singular volume change response that results from the transversely isotropic nature of the Callovo-Oxfordian claystone.

References

Belmokhtar M, Delage P, Ghabezloo S, Conil N (2017a) Thermal volume changes and creep in the Callovo-Oxfordian claystone. Rock Mech Rock Eng 50 (9): 2297 – 2309.

Belmokhtar M, Delage P, Ghabezloo S, Tang AM and Conil N (2017b) Poroelasticity of the Callovo-Oxfordian claystone. Rock Mech Rock Eng 50 (4): 871–889

Blaise T, Barbarand J, Kars M, Ploquin F, Aubourg C, Brigaud B, Cathelineau M, El Albani A, Gautheron C, Izart A, Janots D, Michels R, Pagel M, Pozzi J-P, Boiro MC, Landrein P (2014) Reconstruction of low temperature (<100 °C) burial in sedimentary basins: a comparison of geothermometer in the intra-continental Paris Basin. Mar Pet Geol 53: 71–87.

Braun P, Ghabezloo S, Delage P, Sulem J, Conil N (2019) Determination of Multiple Thermo-Hydro-Mechanical Rock Properties in a Single Transient Experiment: Application to Shales. Rock Mech Rock Eng doi.org/10.1007/s00603-018-1692-x

Conil N, Talandier J, Djizanne H, de La Vaissière R, Righini-Waz C, Auvray C, Morlot C, Armand G (2018) How rock samples can be representative of in situ condition: A case study of Callovo-Oxfordian claystones. J Rock Mech. Geotech. Eng. 10: 613 – 623.

Delage P, Sultan N, Cui YJ (2000) On the thermal consolidation of Boom clay. Can Geotech J 37 (2): 343-354.

Escoffier S, Homand F, Giraud A, Hoteit N, Su K (2005) Under stress permeability determination of the Meuse/Haute-Marne mudstone. Eng Geol 81: 329 – 340.

Favero V, Ferrari A, Laloui L (2016) Thermo-mechanical volume change behaviour of Opalinus Clay. Int J Rock Mech Min Sc. 90: 15 – 25.

Fei Y (1995) Thermal Expansion, American Geophysical Union (AGU): 29 - 44

Gaucher G, Robelin C, Matray JM, Négrel G, Gros Y, Heitz JF, Vinsot A, Rebours H,

Gens A. 2013. On the hydromechanical behaviour of hard soils – weaks rocks. Proc. 15th European Conf. Soil Mech. and Geotech. Eng. (4): 71 – 118, Athens, IOS Press.

McKinstry HA (1965) Thermal expansion of clay minerals. American Mineralogist: Journal of Earth and Planetary Materials 50(1-2): 212-222.Menaceur H, Delage P,

Menaceur H, Delage P., Tang A.M. and Conil N. 2015a. The thermo-mechanical behaviour of the Callovo-Oxfordian claystone. International Journal of Rock Mechanics and Mining Sciences 78: 290-303.

Menaceur H, Delage P, Tang A-M, Conil N (2015b) On the Thermo-Hydro-Mechanical Behaviour of a Sheared Callovo-Oxfordian Claystone Sample with Respect to the EDZ Behaviour. Rock Mech Rock Eng 49(5):1875 – 1888.

Menaceur H., Delage P., Tang A.M. and Talandier J. 2016. The status of water in swelling shales: an insight from the water retention properties of the Callovo-Oxfordian claystone. *Rock Mechanics and Rock Engineering* 49 (12): 4571- 4586.

Mohajerani M, Delage P, Monfared M, Tang A-M, Sulem J, Gatmiri B (2011) Oedometric compression and swelling behaviour of the Callovo-Oxfordian argillite. Int J Rock Mech Min Sci 48: 606–615.

Mohajerani M, Delage P, Sulem J, Monfared M, Tang A-M, Gatmiri B (2014) The Thermal Volume Changes of the Callovo–Oxfordian Claystone. Rock Mech Rock Eng 47: 131–142.

Monfared M, Sulem J, Delage P, Mohajerani M (2011) A Laboratory Investigation on Thermal Properties of the Opalinus Claystone. Rock Mech Rock Eng 44:735–747.
Palciauskas VV, Domenico PA (1982) Characterization of drained and undrained response of thermally loaded repository rocks. Water Resources Research 18(2): 281 - 290
Wileveau Y, Cornet FH, Desroches J, Blumling P (2007) Complete in situ stress determination in an argillite sedimentary formation. Phys Chem Earth 32: 866 – 878.
Yven B, Sammartino S, Geroud Y, Homand F, Villieras F (2007) Mineralogy, texture and porosity of Callovo-Oxfordian claystones of the Meuse/Haute-Marne region (eastern Paris Basin). Mémoires de la Société Géologique de France 178: 73 – 90.
Zhang CL, Conil N, Armand G (2017). Thermal Effects on Clay Rocks for Deep Disposal of High-Level Radioactive Waste. J Rock Mech Geotech Eng 9(3): 463 – 478.

Tables

Table 1. Composition of synthetic pore fluid close to the in-situ one, provided by Andra

	NaCl	$NaHCO_3$	KCl	$CaSO_4$, $2H_2O$	$MgSO_4$, $7H_20$	$CaCl_2$, $2H_2O$	Na_2SO_4
Concentration [g/L_{water}]	1.95	0.13	0.04	0.63	1.02	0.08	0.70

Table 2. Volumetric and linear thermal expansion coefficients of different minerals

Mineral	Mass-fraction P_i (%)	Thermal expansion coefficient α_i (10^{-5} /°C) volumetric	perpendicular	parallel
Muscovite	42	2.48	1.78 [1]	0.35 [1]
Calcite	30	1.4 [2]	0.5	
Quartz	25	3.3 [3]	1.1	
Feldspar	3	1.1 [2]	0.4	

[1]McKinstry (1965), [2]Fei (1995), [3]Palciauskas and Domenico (1982)

Figures

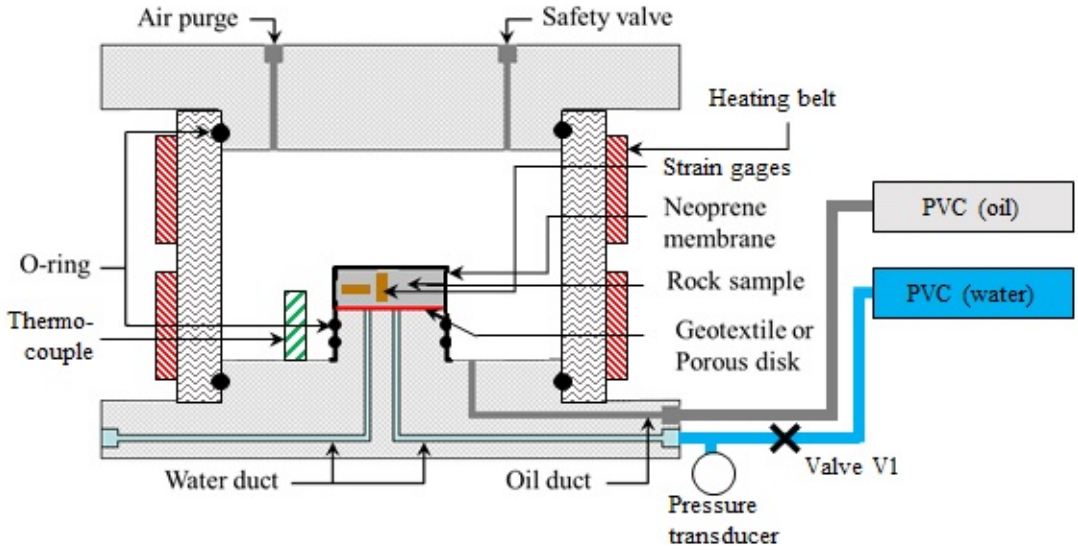

Figure 1. Temperature controlled isotropic compression cell for claystone specimens equipped with strain gauges.

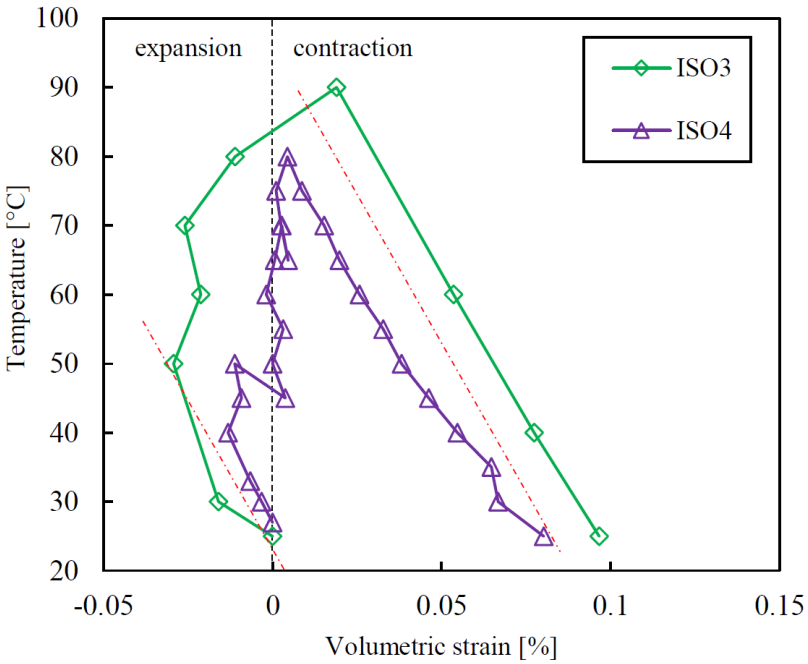

Figure 2. Drained volume changes with respect to temperature changes, measured under constant stress conditions (8 MPa for ISO3 and 10 MPa for ISO4)

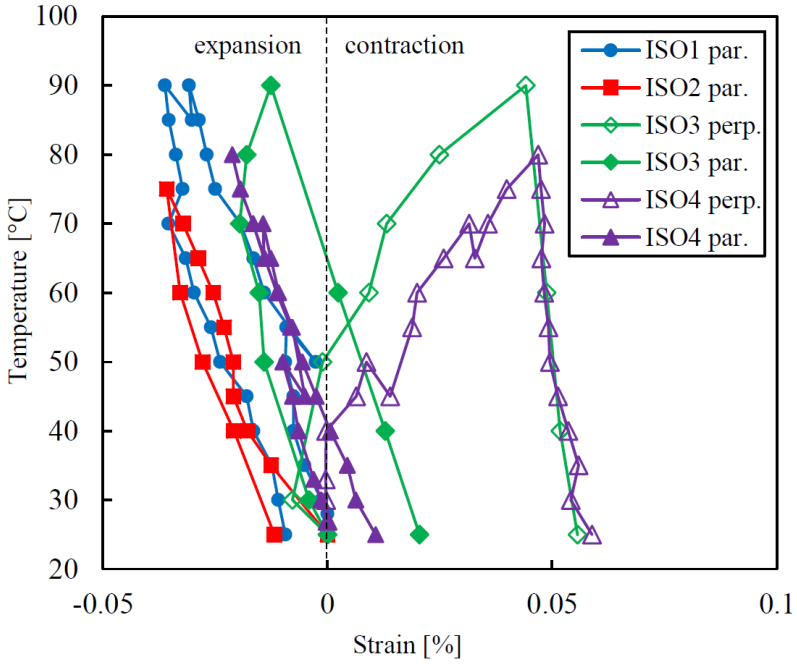

Figure 3. Thermal strain changes parallel to bedding (radial) and perpendicular to bedding (axial) observed under constant confining stress (8 MPa for ISO3 and 10 MPa for ISO4).

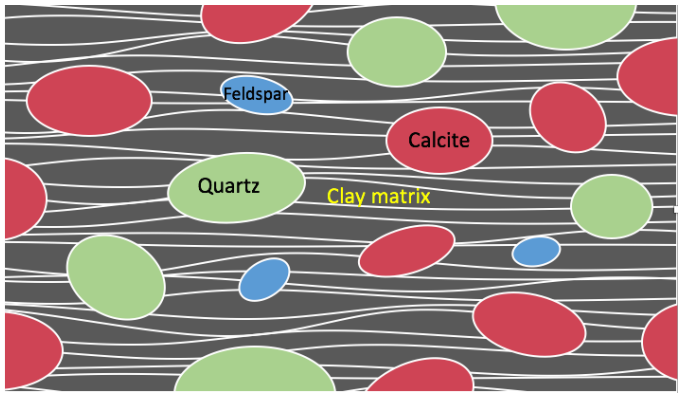

Figure 4. Schematic simplified model of the COx microstructure with granular minerals embedded within the clay matrix